EARTHQUAKE ENGINEERING AND STRUCTURAL DYNAMICS, VOL. 27, 205–223 (1998)

CONTROL OF THE SEISMIC RESPONSE OF A COMPOSITE TALL BUILDING MODELLED BY TWO INTERCONNECTED SHEAR BEAMS

J. ENRIQUE LUCO * AND FRANCISCO C. P. DE BARROS
Department of Applied Mechanics and Engineering Sciences, University of California, San Diego, La Jolla, CA 92093-0411, U.S.A.

SUMMARY

The possibility of controlling the seismic response of tall buildings by use of a structural system consisting of a stiff and lightly damped external structure and a very flexible and moderately damped internal structure connected by stiff links at a few elevations is explored. Optimal damping values for the internal structure are obtained by consideration of the response on the composite structure in the vicinity of its fundamental mode. The resulting optimal damping values depend on the relative stiffness of both structures. Numerical results in the frequency and time domain are used to illustrate the advantages of such a system for seismic excitation. The possibility of using flexible links between the internal and external structures to moderate the required reduction of stiffness in the internal structure is also explored. © 1998 John Wiley & Sons, Ltd.

Earthquake Engng. Struct. Dyn., **27**, 205–223 (1998)

KEY WORDS: control; seismic response; buildings; dynamics

INTRODUCTION

The control of the seismic and wind response of very tall buildings represents a very difficult challenge. In this paper we consider the seismic response of a structural system consisting of a very flexible and moderately damped internal structure connected at several locations along the height of the building to a stiff external structure. The external structure, also called the macro-structure or mega-structure, provides the lateral rigidity to seismic and wind loads, and may consist of a braced frame. The internal structure, also designated as substructure, provides the utilizable space and allows for a significant amount of energy dissipation. Each segment of the internal structure may be several storeys high and is attached to the external structure at the bottom and top of the segment. In this structural system for tall buildings the energy is transferred from the external structure to the internal structure where it is partially dissipated. A system of this type has been considered by Mita and Kaneko[1] and Mita and Feng.[2] In particular, Mita and Kaneko[1] have listed expressions for the optimal values of the natural frequencies and damping ratios for the internal structure derived on the basis of single-degree-of-freedom models for both the internal and external structures. An extension to the case of multi-degree-of-freedom structures has been made through the use of effective mass ratios for the various modes. Mita and Kaneko[1] have also shown the potential of such a system by considering the seismic response of a 20-storey building.

In here, for simplicity and to offer an alternative exploration of the possible optimal configurations of such a system, we model both the internal and external structures as equivalent shear beams connected at several locations along the height by rigid or flexible links. Both the external and internal structures are characterized

* Correspondence to: J. E. Luco, Division of Structural Engineering, U.C.S.D., Serf Building, University Center, La Jolla, CA 92093-0411, U.S.A. E-mail: jeluco@ames.ucsd.edu.

Contract grant sponsor: Shimizu Corporation

CCC 0098–8847/98/030205–19$17·50

Received 22 September 1994
Revised 22 July 1997

by a small amount of hysteretic structural damping. In addition, the internal structure is assumed to have damping devices which provide for additional viscous damping. Although it is recognized that the response of tall buildings involves a significant amount of bending deformation, for the present purposes, it is sufficient to represent the external structure by an equivalent shear beam.

The first objective of this study is to determine the optimal additional viscous damping required to minimize the response of the composite structure as a function of the relative stiffness and relative mass of the internal and external structures and of the height of the composite structure. A second objective is to illustrate the response reductions that can be achieved by such a system. In the case of two shear beams interconnected by several massless rigid links it is found that large response reductions can be obtained if the internal structure can be made sufficiently flexible. Finally, the possibility of using flexible links between the internal and external structures is explored in an attempt at reducing the requirement of an extremely flexible internal structure.

SHEAR BEAMS INTERCONNECTED BY MASSLESS RIGID LINKS

Basic equations for beams with variable properties

As a first model we consider two shear beams ($j=1,2$) of equal total height H interconnected by N massless rigid links spaced at distances ℓ_n ($n=1,N$) as shown in Figure 1. The beams are fixed at the base and free at the top. The first shear beam ($j=1$) represents the external structure while the second beam ($j=2$) represents the internal structure. Each segment of the internal structure may represent a structure several storeys high attached to the external structure at the top and bottom of the segment.

The nth segment of the jth beam is characterized by density ρ_{jn}, cross-sectional area A_{jn} and (complex) shear-wave velocity β_{jn} where

$$\beta_{jn}=\bar{\beta}_{jn}[1+2\mathrm{i}\,\mathrm{sgn}\,(\omega)\xi_{jn}]^{1/2} \tag{1}$$

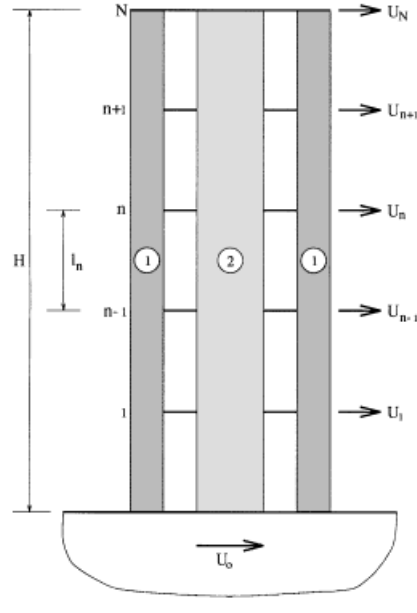

Figure 1. Schematic representation of composite structure showing shear beams connected by rigid links

in which ξ_{jn} is the effective hysteretic damping ratio and ω is the frequency of the excitation. These properties are constant within a given segment but may vary from segment to segment.

For the external structure ($j=1$) we assume that $\xi_{1n}=\xi_{1ns}$ ($n=1,N$) where ξ_{1ns} is a hysteretic damping ratio for the external structure. For the internal structure ($j=2$) we write

$$\xi_{2n}=\xi_{2ns}+\left(\frac{\omega\bar{\ell}}{\bar{\beta}}\right)\left(\frac{\bar{\beta}_{1n}}{\bar{\beta}}\right)\left(\frac{\bar{\beta}}{\bar{\beta}_{2n}}\right)^2\xi_{2nv} \tag{2}$$

where ξ_{2ns} is the intrinsic hysteretic component of the damping in the internal structure. The last term in equation (2) represents the viscous damping added to the internal structure. In equation (2) $\bar{\ell}$ is a length of reference and $\bar{\beta}$ is a shear-wave velocity of reference. The particular normalization of the last term in equation (2) is such that ξ_{2nv} is related to the viscous damping constant c per floor through the relation

$$\xi_{2nv}=\frac{ch}{2\rho_{2n}A_{2n}\bar{\beta}_{1n}\bar{\ell}} \tag{3}$$

where h is the average height of each storey ($h\approx 4\,\mathrm{m}$). Note that in equation (3) the viscous damping constant c in the internal structure has been normalized by $\bar{\beta}_{1n}$ rather than $\bar{\beta}_{2n}$ in an attempt to keep $\bar{\beta}_{2n}$ and ξ_{2nv} as independent variables.

In the case of harmonic vibrations of frequency ω, the equations of motion for the transverse displacement $u_{jn}(x)\,\mathrm{e}^{\mathrm{i}\omega t}$ within the nth segment of the jth beam is given by

$$\frac{\mathrm{d}^2u_{jn}}{\mathrm{d}x^2}+\left(\frac{\omega}{\beta_{jn}}\right)^2u_{jn}=0\quad(j=1,2) \tag{4}$$

where x is a local co-ordinate ($0\leqslant x\leqslant\ell_n$). The end conditions for the nth segment—which also correspond to continuity conditions for the whole structure—are

$$u_{jn}(0)=U_{n-1}\quad(j=1,2) \tag{5a}$$

$$u_{jn}(\ell_n)=U_n\quad(j=1,2) \tag{5b}$$

where U_{n-1} and U_n are the displacements at the bottom and top of the nth segment, respectively. The general solution to equation (4) with end conditions (5a) and (5b) is

$$u_{jn}(x)=\{U_n\sin[\omega x/\beta_{jn}]+U_{n-1}\sin[\omega(\ell_n-x)/\beta_{jn}]\}\csc\alpha_{jn},\quad(0\leqslant x\leqslant\ell_n)\quad(j=1,2) \tag{6}$$

where $\alpha_{jn}=\omega\ell_n/\beta_{jn}$.

The combined total shear force $S_n(x)\mathrm{e}^{\mathrm{i}\omega t}$ at level x within the nth segment is given by

$$S_n(x)=\rho_{1n}A_{1n}\beta_{1n}^2u'_{1n}(x)+\rho_{2n}A_{2n}\beta_{2n}^2u'_{2n}(x) \tag{7}$$

where the primes denote differentiation with respect to x. In particular, the total normalized shear forces $\bar{S}_n$ and $\bar{S}_{n-1}$ at the top and bottom of the nth segment correspond to

$$\bar{S}_n=S_n(\ell_n)/(\bar{\rho}\bar{A}\,\bar{\beta}^2/\bar{\ell})=b_nU_n-a_nU_{n-1} \tag{8a}$$

$$\bar{S}_{n-1}=S_n(0)/(\bar{\rho}\bar{A}\,\bar{\beta}^2\bar{\ell})=a_nU_n-b_nU_{n-1} \tag{8b}$$

where $S_n(\ell_n)$ and $S_n(0)$ are the actual shear forces at the top and bottom of the nth segment. The parameters $\bar{\rho}$ and $\bar{A}$ are a density and cross-sectional area of reference and

$$a_n = \left[\left(\frac{\rho_{1n}A_{1n}\beta_{1n}^2}{\bar{\rho}\bar{A}\,\bar{\beta}^2}\right)\alpha_{1n}\csc\alpha_{1n} + \left(\frac{\rho_{2n}A_{2n}\beta_{2n}^2}{\bar{\rho}\bar{A}\,\bar{\beta}^2}\right)\alpha_{2n}\csc\alpha_{2n}\right]\left(\frac{\bar{\ell}}{\ell_n}\right) \tag{9a}$$

$$b_n = \left[\left(\frac{\rho_{1n}A_{1n}\beta_{1n}^2}{\bar{\rho}\bar{A}\,\bar{\beta}^2}\right)\alpha_{1n}\cot\alpha_{1n} + \left(\frac{\rho_{2n}A_{2n}\beta_{2n}^2}{\bar{\rho}\bar{A}\bar{\beta}^2}\right)\alpha_{2n}\cot\alpha_{2n}\right]\left(\frac{\bar{\ell}}{\ell_n}\right) \tag{9b}$$

Equations (8a) and (8b) can also be written in the form

$$\begin{Bmatrix}\bar{S}_n\\ U_n\end{Bmatrix} = [T_n]\begin{Bmatrix}\bar{S}_{n-1}\\ U_{n-1}\end{Bmatrix} \tag{10}$$

where the transfer matrix $[T_n]$ is given by

$$[T_n] = \begin{bmatrix} b_n/a_n & (b_n^2 - a_n^2)/a_n \\ 1/a_n & b_n/a_n \end{bmatrix} \tag{11}$$

Succesive application of equation (10) leads to

$$\begin{Bmatrix}\bar{S}_N\\ U_N\end{Bmatrix} = [\gamma(\omega)]\begin{Bmatrix}\bar{S}_0\\ U_0\end{Bmatrix} \tag{12}$$

where $U_0\,e^{i\omega t}$ represents the prescribed displacement of the base and

$$[\gamma(\omega)] = [T_N][T_{N-1}]\ldots[T_1] \tag{13}$$

is total transfer matrix.

Applying the boundary condition $\bar{S}_N = 0$ at the top of the composite structure leads to

$$\bar{S}_0 = -\left(\frac{\gamma_{12}}{\gamma_{11}}\right)U_0 \tag{14a}$$

and

$$U_N = \left(\gamma_{22} - \frac{\gamma_{12}\,\gamma_{21}}{\gamma_{11}}\right)U_0 \tag{14b}$$

from where all of the remaining link displacements $U_n(n = 1, N-1)$ can be determined by using equation (10). The displacements $u_{jn}(x)$ and the total shear forces $S_n(x)$ within each segment can then be obtained by using equations (6) and (7). Results in the time domain can be obtained by Fourier synthesis of the frequency-domain response for a prescribed ground motion U_0.

Uniform beams connected by equally spaced links

In the particular case of uniform shear beams with equally spaced massless rigid links spaced at $\ell_n = \ell = H/N$ the terms a_n and b_n are independent of n, i.e. $a_n = a$ and $b_n = b$ $(n = 1, N)$, and the previous formulation can be simplified. The continuity equations for the first $(N-1)$ links and the end condition at the top of the structure can be written in the form

$$aU_{n+1} - bU_n = bU_n - aU_{n-1} \quad (n = 1, N-1) \tag{15a}$$

$$bU_N - aU_{N-1} = 0 \tag{15b}$$

where $U_0 e^{i\omega t}$ represents the motion of the base. Using a standard method it can be shown that the solution to equations (15a) and (15b) for a prescribed motion of the base is given by

$$U_n = U_0 \frac{\cos[(N-n)\alpha]}{\cos(N\alpha)} \quad (n = 1, N) \tag{16}$$

where $\cos\alpha = b/a$ or, equivalently,

$$\sin\left(\frac{\alpha}{2}\right) = \left[\frac{1-(a/b)}{2}\right]^{1/2} \tag{17}$$

To determine α we select $\mathrm{Re}\,\alpha \geqslant 0$.

We note that if $\omega\ell/\bar{\beta}_1 \ll 1$ and $\omega\ell/\bar{\beta}_2 \ll 1$ then α can be approximated by

$$\alpha \approx \frac{\omega\ell}{\beta_e}(1 - i\xi_e) \tag{18}$$

where

$$\beta_e = \sqrt{\mu_1 \bar{\beta}_1^2 + \mu_2 \bar{\beta}_2^2} \tag{19}$$

and

$$\xi_e = \mu_1 \left(\frac{\bar{\beta}_1}{\beta_e}\right)^2 \xi_1 + \mu_2 \left(\frac{\bar{\beta}_2}{\beta_e}\right)^2 \xi_2 \tag{20}$$

in which μ_j $(j = 1, 2)$ represent the mass ratios

$$\mu_j = \frac{\rho_j A_j}{\rho_1 A_1 + \rho_2 A_2} \quad (j = 1, 2) \tag{21}$$

The terms β_e and ξ_e represent, respectively, the effective shear-wave velocity and the effective damping ratio at low frequencies. Finally, if $\bar{\beta}_j/\beta_e \gg \pi/2N$ $(j = 1, 2)$ the fundamental frequency of the composite structure can be approximated by $\omega_1 \approx \pi\beta_e/2N\ell$. The subscript n affecting $\bar{\beta}_{jn}$, ρ_{jn}, A_{jn} and ξ_{jn} have been dropped from equations (19)–(21).

Equation (20) indicates that if $\bar{\beta}_1/\beta_e \gg \pi/2N$ and $\bar{\beta}_2/\beta_e \gg \pi/2N$ then the contribution of ξ_2 to the effective damping ξ_e in the vicinity of the fundamental frequency is not amplified. To obtain significant amplification of the additional damping ξ_2 it is necessary to render equation (20) invalid by selecting $\bar{\beta}_2/\beta_e \leqslant \pi/2N$. In particular, to tune the fundamental frequency of the internal structure $(\pi\bar{\beta}_2/\ell)$ to the fundamental frequency of the external structure $(\pi\bar{\beta}_1/2N\ell)$ it is necessary to select $\bar{\beta}_2/\bar{\beta}_1 = (1/2N)$. For N large, $\bar{\beta}_2/\bar{\beta}_1 \ll 1$, $\beta_e \approx \sqrt{\mu_1}\,\bar{\beta}_1$ and $\bar{\beta}_2/\beta_e \approx 1/(2N\sqrt{\mu_1})$. Thus, to obtain an amplification of the damping ξ_2 of the internal structure this structure must be made very flexible.

Infinitely tall structures connected by rigid links

A further simplification can be obtained for the case of two uniform infinitely tall shear beams connected by equally spaced massless rigid links. In this case, equation (15a) applies for all $n \geqslant 1$ and the solution for the absolute displacements at the links is given by

$$U_n = U_0 \exp(-in\alpha) \tag{22}$$

where α $(\mathrm{Re}\,\alpha > 0)$ is defined by equation (17). Equation (22) indicates that the optimal choice of parameters to obtain a large attenuation along the height of the structure should render $|\mathrm{Im}\,\alpha|$ as large as possible $(\mathrm{Im}\,\alpha \leqslant 0)$.

Again, if $\omega\ell/\bar{\beta}_1 \ll 1$ and $\omega\ell/\bar{\beta}_2 \ll 1$, α can be approximated by equation (18). In this case,

$$U_n e^{i\omega t} = U_0 e^{i\omega(t-n\ell/\beta_e)} e^{-\omega n\ell\xi_e/\beta_e} \tag{23}$$

indicating that the motion propagates upwards with effective velocity β_e and effective damping ratio ξ_e.

Numerical results in the frequency domain

To illustrate the effects of the relative stiffness between the two structures on the response of the composite structure as well as the effects of the additional viscous damping, we consider the case of two uniform shear beams interconnected by equally spaced massless rigid links.

In the examples that follow it will be assumed that $\bar{\ell} = \ell = \ell_n = H/N = 40\,\text{m}$ so that each segment is approximately 10-storey high. In addition, $\xi_{1ns} = \xi_{2ns} = 0{\cdot}02$, $\rho_1 A_1/\rho_2 A_2 = 1/3$ ($\mu_1 = 1/4$, $\mu_2 = 3/4$), $\bar{\rho}\bar{A} = \rho_1 A_1 + \rho_2 A_2$ and $\bar{\beta} = \beta_e$ where $\beta_e = 160\,\text{m/sec}$ is defined by equation (19). In this case, values of $\bar{\beta}_2/\beta_e = 1{\cdot}0$, $0{\cdot}5$, $0{\cdot}2$, $0{\cdot}1$ and $0{\cdot}05$ correspond to $\bar{\beta}_1/\beta_e = 1{\cdot}0$, $1{\cdot}803$, $1{\cdot}970$, $1{\cdot}992$ and $1{\cdot}998$, respectively. Results for $N = 10$, 5 and 2 will be presented which can be considered representative for structures of 100, 50 and 20-storeys.

To estimate a realistic range of values for the measure of added damping ξ_{2nv} we consider the results of Yokota *et al.*,[3] who have developed viscous damping surfaces that can be implemented on the walls of the internal structure. Using $5{\cdot}5\,\text{m}^2$ of such damping surfaces per floor leads to $c = 5{\cdot}5 \times 10^7\,\text{N sec/m}$. If we take $\bar{\beta}_{1n} \approx 300\,\text{m/sec}$, $\bar{\ell} = 40\,\text{m}$, $\rho_{2n} A_{2n} \bar{\ell} = 10^7\,\text{kg}$ and $h = 4\,\text{m}$, we obtain $\xi_{2nv} = \xi_{2v} = 0{\cdot}037$. Thus, we will consider values for ξ_{2v} in the range $0{\cdot}0$–$0{\cdot}10$.

Figures 2(a)–2(c) show the amplitudes of the transfer functions $U_N(\omega)/U_0$ for the absolute displacement at the top of the composite structure as a function of the dimensionless frequency $a_0 = (\omega\bar{\ell}/\bar{\beta})$ for different values of the ratio $\bar{\beta}_2/\beta_e$ for the case $N = 10$. Figures 2(a)–2(c) correspond to added viscous damping values of $\xi_{2v} = 1$, 5 and 10 per cent, respectively. Figure 2(a) indicates that when the added viscous damping is small ($\xi_{2v} = 1\%$) then the peak amplitude of the transfer function U_N/U_0 in the vicinity of the first mode ($a_0 = \omega\bar{\ell}/\bar{\beta} \approx 0{\cdot}157$ for $N = 10$) decreases significantly as the internal structure becomes softer. For $\bar{\beta}_2/\beta_e = 0{\cdot}05$ the peak amplitude has been reduced by a factor of the order of 6. The results in Figure 2(b) indicate that when the added viscous damping is more significant ($\xi_{2v} = 5\%$) then reductions of the peak amplitude are obtained as $\bar{\beta}_2/\beta_e$ is reduced from $1{\cdot}0$ to $0{\cdot}10$. Further reductions of $\bar{\beta}_2/\beta_e$ beyond $\bar{\beta}_2/\beta_e = 0{\cdot}10$ do not lead to additional reductions of the peak response in the fundamental mode. For a larger amount of added viscous damping ($\xi_{2v} = 10$ per cent, Figure 2(c)) no additional reductions of the response are obtained by softening the internal structure beyond $\bar{\beta}_2/\beta_e \approx 0{\cdot}20$.

The dependence of the amplitude of the transfer function $U_N(\omega)/U_0$ on the added viscous damping (ξ_{2v}) in the vicinity of the first mode of a composite structure with $N = 10$ is presented in Figures 3(a), 3(b) and 3(c) for values of $\bar{\beta}_2/\beta_e = 0{\cdot}05$, $0{\cdot}10$ and $0{\cdot}20$, respectively. It is apparent from Figures 3(a) that an optimal viscous damping exists ($\xi_{2v} \approx 0{\cdot}4\%$) when $\bar{\beta}_2/\beta_e = 0{\cdot}05$. In this case, the peak amplitude of the transfer function is of the order of $3{\cdot}1$ which is significantly lower than the corresponding peak value of $15{\cdot}9$ (Table I) for $\bar{\beta}_2/\beta_e = 0{\cdot}05$ and $\xi_{2v} = 0$, i.e. when no added viscous damping is introduced. The peak amplitude of $3{\cdot}1$ is also considerably lower than the peak amplitude of $30{\cdot}0$ for $\bar{\beta}_2/\beta_e = 1{\cdot}0$ and $\xi_{2v} = 0{\cdot}4$ per cent and of $31{\cdot}83$ for $\bar{\beta}_2/\beta_e = 1{\cdot}0$ and $\xi_{2v} = 0$, i.e. for a standard structure with no added viscous damping. The results in Figure 3(b) for $\bar{\beta}_2/\beta_e = 0{\cdot}1$ also show the existence of an optimal viscous damping ($\xi_{2v} \approx 1{\cdot}6$ per cent). In this case, the peak amplitude of the transfer function is only reduced to a value of about $9{\cdot}76$. Finally, Figure 3(c) for $\bar{\beta}_2/\beta_e = 0{\cdot}2$ shows that if there is an optimal value for the added viscous damping it must be fairly high ($\xi_{2v} > 10$ per cent).

The effects of $\bar{\beta}_2/\beta_e$ and ξ_{2v} on the peak amplitude of the transfer function $U_N(\omega)/U_0$ in the vicinity of the fundamental mode are shown in Figures 4(a), 4(b) and 4(c) for the cases $N = 10$ (100-storeys), $N = 5$ (50-storeys) and $N = 2$ (20-storeys), respectively. The results in Figures 4(a), 4(b) and 4(c) indicate that when $\xi_{2v} > 6$ per cent there is little gain in softening the internal structure beyond a certain point. If the internal structure can be made significantly softer than the external structure then large response reductions can be

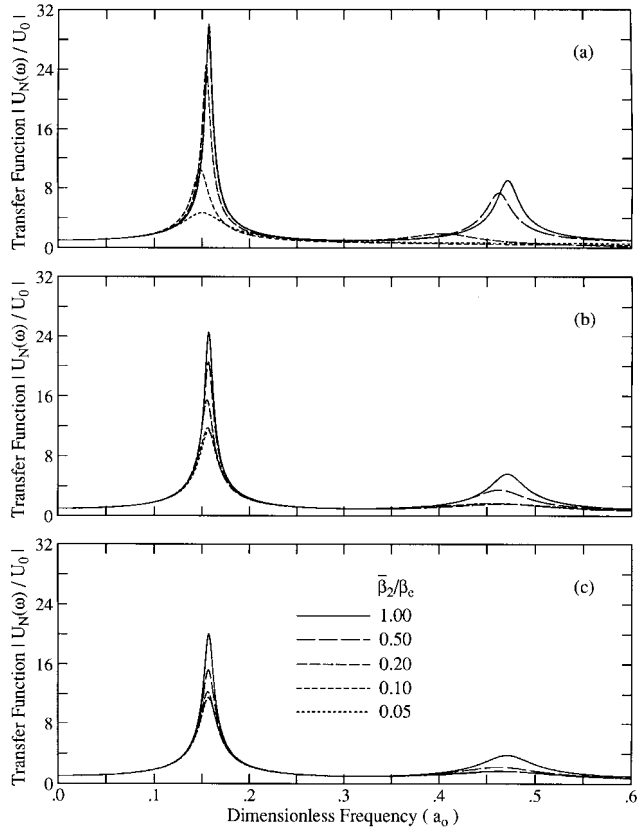

Figure 2. Amplitude of the transfer function $U_N(\omega)/U_0$ for the absolute displacement at the top of a 100-storey structure ($N = 10$) for different values of $\bar{\beta}_2/\beta_e$. Frames (a), (b) and (c), correspond to added viscous damping values of $\xi_{2v} = 0{\cdot}01$, $0{\cdot}05$ and $0{\cdot}10$, respectively

Table I. Optimal added viscous damping ξ_{2v} and corresponding effective damping $\bar{\xi}_e$ for different values of $\bar{\beta}_2/\beta_e$. Comparison of peak amplitudes of the transfer function U_N/U_0 for different values of $\bar{\beta}_2/\beta_e$ and ξ_{2v}

N	No. of storeys	$\bar{\beta}_2/\beta_e$	Optimal ξ_{2v} (%)	Effective damping $\bar{\xi}_e$ (%)	Peak amplitude $(\xi_{2v})_{opt.}$	Peak amplitude $\xi_{2v} = 0$	Peak amplitudes $\bar{\beta}_2/\beta_e = 1{\cdot}0$	
							$(\xi_{2v})_{opt.}$	$\xi_{2v} = 0$
2	20	0·20	1·4	33·9	2·13	12·09	22·55	31·83
5	50	0·15	1·8	10·1	6·07	23·62	26·27	31·83
		0·10	0·8	19·9	3·08	16·08	29·09	31·83
10	100	0·10	1·6	6·4	9·76	26·63	29·09	31·83
		0·05	0·4	19·6	3·10	15·87	31·09	31·83

obtained by using a small amount of added viscous damping. It is also apparent from Figures 4(a)–4(c) that for a given softening of the internal structure, i.e. for a given value of $\bar{\beta}_2/\beta_e$, larger response reductions are obtained for $N = 2$ than for $N = 10$.

The optimal damping values ξ_{2v} that minimize the peak amplitude of the transfer function for the absolute displacement at the top of 100, 50, and 20-storey structures in the vicinity of the fundamental frequency can

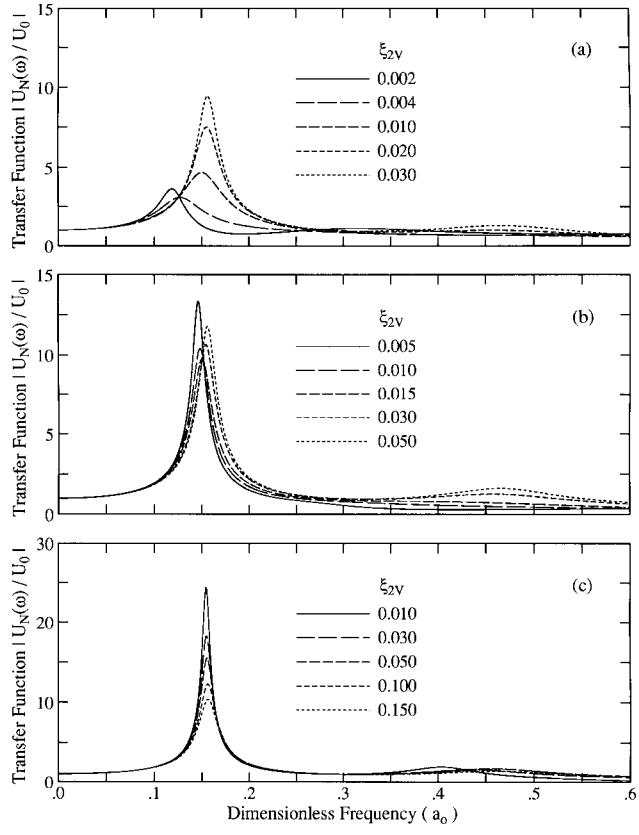

Figure 3. Amplitude of the transfer function $U_N(\omega)/U_0$ for the absolute displacement at the top of a 100-storey structure ($N = 10$) for different values of the added viscous damping ξ_{2v}. Frames (a), (b) and (c), correspond to relative stiffnesses of $\bar{\beta}_2/\beta_e = 0{\cdot}05$, $0{\cdot}10$ and $0{\cdot}2$, respectively

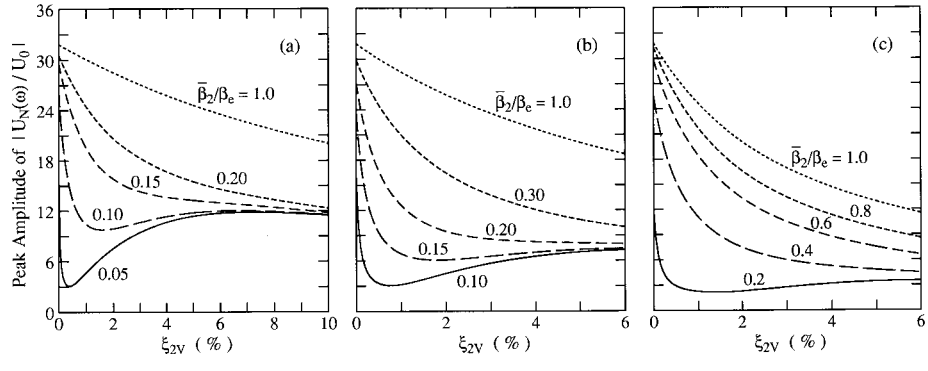

Figure 4. Peak amplitude of the transfer function $U_N(\omega)/U_0$ in the vicinity of the fundamental frequency as a function of the added viscous damping ξ_{2v} for different values of the relative stiffness $\bar{\beta}_2/\beta_e$. (a), (b) and (c) correspond to 100, 50 and 20-storey buildings ($N = 10$, 5 and 2), respectively

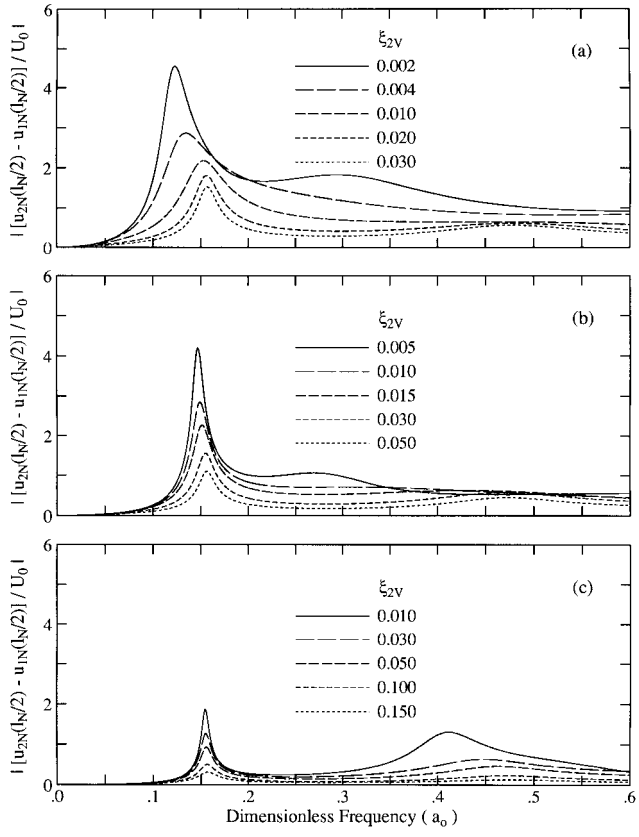

Figure 5. Amplitude of the transfer function $(u_{2N} - u_{1N})/U_0$ at the centre of the upper segment of a 100-storey structure ($N = 10$) for different values of the added viscous damping ξ_{2v}. (a), (b) and (c) correspond to $\bar{\beta}_2/\beta_e = 0{\cdot}05$, $0{\cdot}10$ and $0{\cdot}2$, respectively

be obtained from Figures 4(a)–4(c). Some of the optimal values of ξ_{2v} are listed in Table I for several values of $\bar{\beta}_2/\beta_e$. Table I also includes a comparison of the peak amplitudes of the transfer function $U_N(\omega)/U_0$ in the vicinity of the fundamental frequency of the structure for other values of $\bar{\beta}_2/\beta_e$ and/or ξ_{2v}. It is apparent that the strategy of using a very flexible internal structure with an appropriate amount of added viscous damping may lead to very large reductions of the overall response in the vicinity of the first mode of the structure.

Another way to describe the effectiveness of the resulting optimal composite structure is to consider the effective modal damping ratio $\bar{\xi}_e$ for the complete structure. The values for $\bar{\xi}_e$ obtained from the width of the transfer fuctions in the vicinity of the fundamental frequency are listed in Table I and range from 6·4 to 33·9 per cent depending on the number of storeys and on $\bar{\beta}_2/\bar{\beta}_e$.

We now turn our attention to the relative displacement of the internal structure with respect to the external structure. Clearly, the response reductions obtained for the external structure are not acceptable if they result in large deformations of the internal structure. Figures 5(a)–5(c) show the amplitude of the transfer function $[u_{2N}(\ell_N/2) - u_{1N}(\ell_N/2)]/U_0$ at the centre ($x = \ell_N/2$) of the upper segment of the structure as a function of the dimensionless frequency $a_0 = \omega\bar{\ell}/\bar{\beta}$ for $N = 10$. The results for $\bar{\beta}_2/\beta_e = 0{\cdot}05$, $0{\cdot}10$ and $0{\cdot}20$ are shown for different values of the added viscous damping ξ_{2v}. The results indicate that the relative displacement in the vicinity of the fundamental mode increases as $\bar{\beta}_2/\beta_e$ and ξ_{2v} decrease.

Figures 6(a)–6(c) show the peak amplitudes of the transfer function $[u_{2N}(\ell_N/2) - U_{N-1}]/U_0$ in the vicinity of the fundamental frequency of the composite structure as a function of the added viscous damping ξ_{2v} for

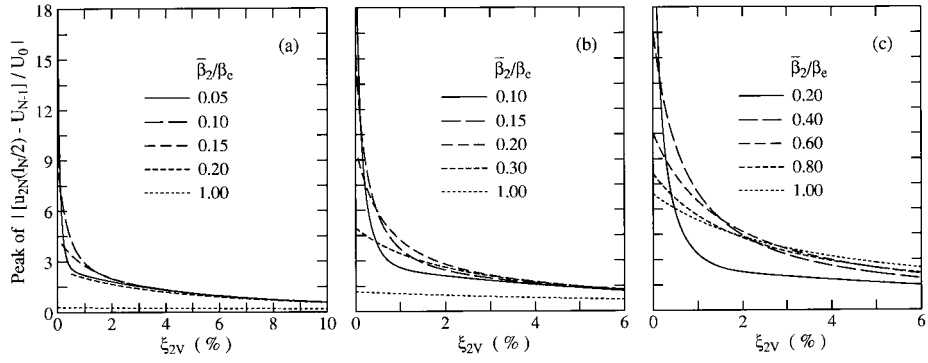

Figure 6. Peak amplitude of the transfer function $[u_{2N}(\ell_N/2) - U_{N-1}]/U_0$ in the vicinity of the fundamental frequency as a function of the added viscous damping ξ_{2v} for different values of the relative stiffness $\bar{\beta}_2/\beta_e$. (a), (b) and (c) correspond to 100, 50 and 20-storey buildings ($N = 10$, 5 and 2), respectively

different values of $\bar{\beta}_2/\beta_e$. This transfer function measures the deformation of the upper segment of the internal structure ($j = 2$). The results in Figures 6(a), 6(b) and 6(c) correspond, respectively, to $N = 10$ (100-storey building), $N = 5$ (50-storey building) and $N = 2$ (20-storey building). These results indicate that significant deformations of the internal structure may be obtained when $\bar{\beta}_2/\beta_e$ and ξ_{2v} are small. If $\xi_{2v} > 1{\cdot}5$ per cent, the deformation of the internal structure is relatively independent of $\bar{\beta}_2/\beta_e$ (at least for $\bar{\beta}_2/\beta_e < 0{\cdot}3$) for $N = 10$ and $N = 5$. For $N = 2$, this result applies if $0{\cdot}4 \leqslant \bar{\beta}_2/\beta_e \leqslant 1{\cdot}0$. To avoid relatively large deformations of the internal structure it seems necessary to use added viscous damping ratios of at least $\xi_{2v} = 0{\cdot}01$ to $0{\cdot}02$.

Results in the time domain

Next we consider some results in the time domain obtained by using as excitation a filtered version of the NS El Centro 1940 strong motion record (peak acceleration = 3·41 m/sec^2, peak velocity = 0·35 m/sec). In all cases, the structures are characterized by $\xi_{1ns} = \xi_{2ns} = 2$ per cent, $\mu_1 = 0{\cdot}25$, $\mu_2 = 0{\cdot}75$, $\bar{\ell} = \ell_n = 40$ m and $\bar{\beta} = \beta_e = 160$ m/sec. Figures 7, 8 and 9 show the variation with height of the peak absolute accelerations and peak relative displacements with respect to the base for both the external and the internal structures for buildings with 20, 50 and 100-storeys, respectively. For each total height, three cases corresponding to different values for the relative stiffness $\bar{\beta}_2/\bar{\beta}_e$ and the added viscous damping ξ_{2v} are considered (Table II).

Case 1 corresponds to a composite structure with the optimum added damping ξ_{2v} for a given relative stiffness $\bar{\beta}_2/\beta_e$. In Case 2 the parameter $\bar{\beta}_2/\beta_e$ is kept the same as in Case 1 but the added damping is doubled. Finally, in Case 3 no viscous damping ($\xi_{2v} = 0$) is added and the internal and external structures have the same shear-wave velocities ($\bar{\beta}_1 = \bar{\beta}_2 = \beta_e = 160$ m/sec) and structural damping ratios ($\xi_{1s} = \xi_{2s} = 2$ per cent). The results for Case 3 can be thought to correspond to those for a standard structure.

The results in Figures 7–9 show the significant advantages of using a composite structure consisting of a very flexible internal structure and a stiffer external structure. In this case, reductions of the peak response by factors larger than two can be obtained in the upper-half of the building. However, the relative displacement of the internal structure with respect to the base may exceed the corresponding displacement for a standard structure in the lower-half of the building. Comparison of the results for Cases 1 and 2 indicate that increasing the added damping beyond the optimal value may increase slightly the response of the external structure but it may have beneficial effects on the displacement response over portions of the internal structure.

The reductions in response shown in Figures 7–9 are obtained at the expense on some deformation of the internal structure. Figure 10 shows the peak values of the internal relative displacement $[u_2(x) - u_1(x)]$ along the height of the building for Cases 1 and 2 [in Case 3 the relative displacements $u_2(x) - u_1(x)$ are zero]. If the optimal added damping is used, then peak relative displacements between floors of about 3 to 4 cm (20 cm/5 = 4 cm) are obtained. If the added damping is doubled the peak inter-floor displacements

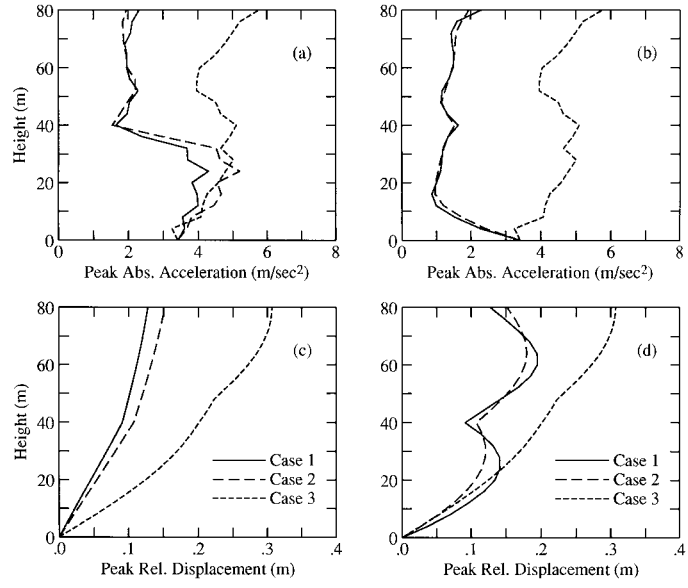

Figure 7. Distribution of peak absolute accelerations (m/sec^2) and peak relative displacements (m) along the height of the external ((a), (c)) and internal ((b), (d)) structures in a composite 20-storey building

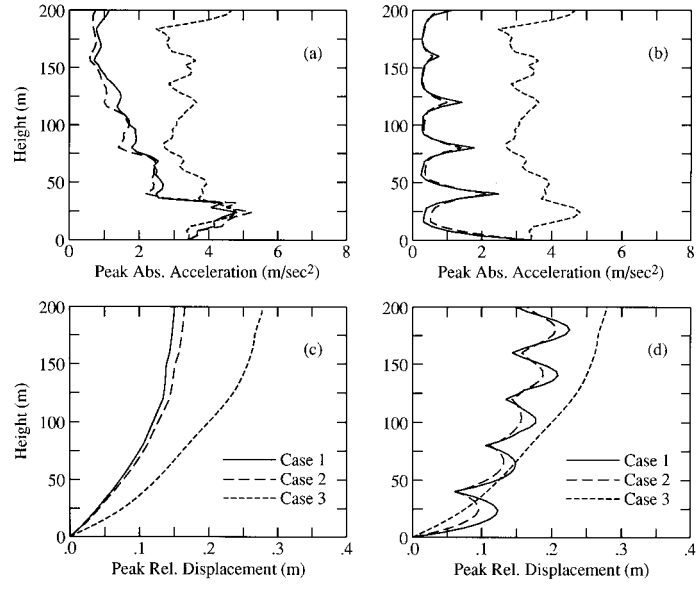

Figure 8. Distribution of peak absolute accelerations (m/sec^2) and peak relative displacements (m) along the height of the external ((a), (c)) and internal ((b), (d)) structures in a composite 50-storey building

are reduced to about 2–3 cm. In any case, the lateral displacements amount to less than 1 per cent of the interstorey height of 4 m.

A comparison of the time histories for the absolute acceleration and relative displacement at the top of a 50-storey structure subjected to the NS El Centro 1940 excitation is shown in Figure 11. The comparisons

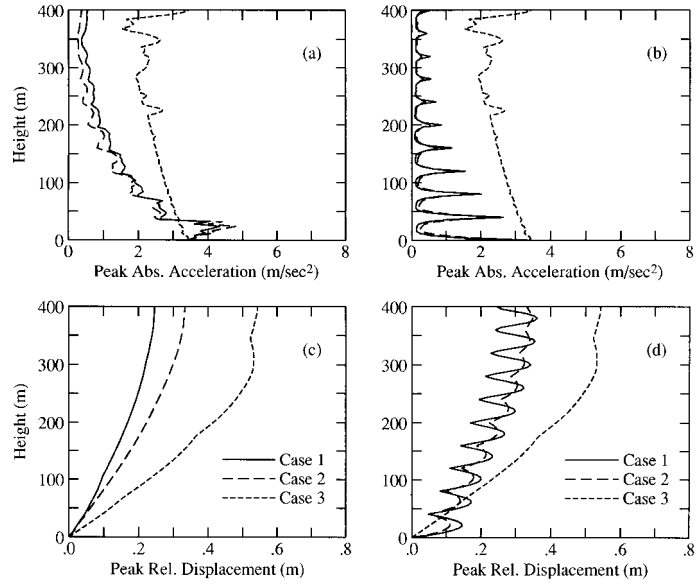

Figure 9. Distribution of peak absolute accelerations (m/sec^2) and peak relative displacements (m) along the height of the external ((a), (c)) and internal ((b), (d)) structures in a composite 100-storey building

Table II. Peak values of the absolute acceleration, absolute velocity and displacement relative to the base at the top of the building. Peak values of the relative displacement between the internal and external structures at the centre of the upper 10-storey segment of the building (El Centro Excitation)

Case	$\bar{\beta}_2/\beta_e$	ξ_{2v}	Abs. accel. (m/sec^2) $\ddot{U}_N$	Abs. veloc. (m/sec) $\dot{U}_N$	Rel. displ. (cm) $U_N - U_0$	Rel. displ. (cm) $u_2 - u_1$
			(a) 20-storey building			
1	0·20	1·4%	2·31	0·36	12·7	15·7
2	0·20	2·8%	1·95	0·45	15·2	10·6
3	1·00	0·0%	5·77	1·12	30·7	0·0
			(b) 50-storey building			
1	0·10	0·8%	1·14	0·25	15·0	13·2
2	0·10	1·6%	0·76	0·25	16·6	9·3
3	1·00	0·0%	4·68	0·59	27·8	0·0
			(c) 100-storey building			
1	0·05	0·4%	0·56	0·16	24·7	21·0
2	0·05	0·8%	0·38	0·17	33·3	16·3
3	1·00	0·0%	3·45	0·46	54·3	0·0

are made between a standard structure with $\bar{\beta}_2/\beta_e = 1{\cdot}0$ and $\xi_{2v} = 0{\cdot}0$ (Case 3) and a composite structure with $\bar{\beta}_2/\beta_e = 0{\cdot}1$ and $\xi_{2v} = 0{\cdot}8$ per cent (Case 1). Also shown in Figure 11 is the time history for the relative displacement $[u_2 - u_1]$ between the internal and external structures at the centre of the upper 10-storey segment of the structure.

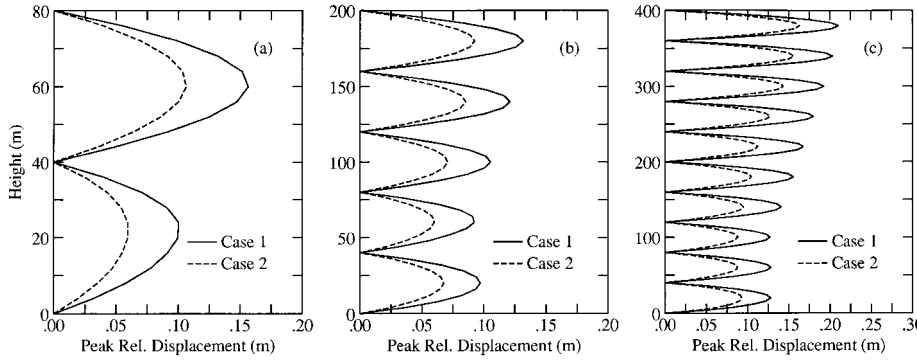

Figure 10. Distribution of peak internal relative displacements $[u_2(x) - u_1(x)]$ along the height of (a) 20, (b) 50 and (c) 100-storey composite buildings for El Centro excitation

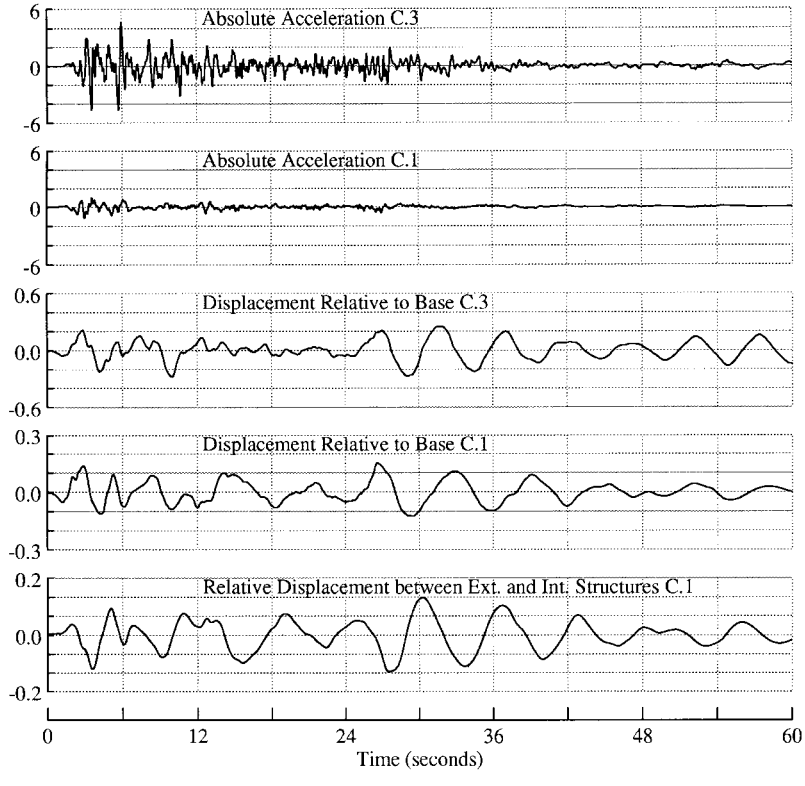

Figure 11. Comparison of time histories for the absolute acceleration (m/sec^2) and relative displacement (m) at the top of a 50-storey standard structure (Case 3, $\bar{\beta}_2/\beta_e = 1.0$, $\xi_{2v} = 0{\cdot}0$) and a composite structure (Case 1, $\bar{\beta}_2/\beta_e = 0{\cdot}1$, $\xi_{2v} = 0{\cdot}8$ per cent) for El Centro excitation. The figure also shows the relative displacement (m) between internal and external structures at the centre of the upper segment of the composite structure

A summary of the peak absolute accelerations, peak absolute velocities and peak displacements relative to the base at the top of 20, 50 and 100-storey buildings for El Centro 1940 excitation is presented in Table II. Also listed are the peak values of the relative displacememt $[u_2 - u_1]$ at the centre of the upper 10-storey segment of the structure. At the top of the structure, the peak relative displacements with respect to the base

and peak absolute velocities are reduced by factors of 2–3. The reductions of the absolute peak acceleration correspond to factors of 2, 4 and 6 for 20, 50 and 100-storey structures, respectively. The local deformations of the internal structure increase as the height of the building increases as a result of the required increased flexibility of the internal structure and of the corresponding lower optimal damping ratios.

SHEAR BEAMS INTERCONNECTED BY FLEXIBLE LINKS

The previous discussion for shear beams interconnected by rigid links indicates that substantial response reductions can be obtained provided that the internal structure can be made sufficiently flexible so that the characteristic frequencies of the internal structure can be made comparable to those of the external structure. Since the length of each internal substructure is much smaller than the total height of the building a large stiffness reduction is required. In here we explore the possibility of using flexible links between the two structures to limit the required stiffness reduction of the internal structure. Dampers can also be placed at the connections between the two structures.

The problem considered here has some relation to the model of two uniform shear beams interconnected by one damped elastic link used by Gurley *et al.*[4] to study the coupling of tall adjacent buildings in a attempt to control the response to wind excitation. The present approach differs from that of Gurley *et al.*[4] in that: (i) multiple links are considered, (ii) the structures are damped, (iii) the formulation admits non-uniform segments, (iv) seismic instead of wind excitation is considered, (v) response in the frequency and time domain are presented rather than rms results and (vi) the emphasis is on the optimal choice of links connecting a very stiff external structure with a very flexible internal structure rather than the optimal choice of a link between two adjacent structures of similar stiffnesses.

Basic equations

Next, we consider a slightly more complex model of the composite structure in which the links connecting the two shear beams are flexible and are characterized by the complex stiffness $k_n^* = (k_n + \mathrm{i}\omega c_n)$ where k_n and c_n are the link stiffness and viscous damping constants, respectively. In addition, we consider masses m_{1n} and m_{2n} at the connections between the shear beams (Figure 12). In this case, the displacements of the shear beams ($j = 1, 2$) at the links are denoted by U_{1n} and U_{2n} ($n = 0, N$). The displacements within each shear beam are given by

$$u_{jn}(x) = \{U_{jn} \sin [\alpha_{jn} x/\ell_n] + U_{j(n-1)} \sin [\alpha_{jn}(\ell_n - x)/\ell_n]\} \csc \alpha_{jn}, \quad (0 \leqslant x \leqslant \ell_n) \quad (j = 1,2;\ n = 1, N) \tag{24}$$

where x is a local co-ordinate within the nth segment and $\alpha_{jn} = \omega \ell_n / \beta_{jn}$.

The shear force $S_{jn}(x)$ in each beam within the nth segment is given by

$$S_{jn}(x) = \omega \rho_{jn} A_{jn} \beta_{jn} \{U_{jn} \cos [\alpha_{jn} x/\ell_n] - U_{j(n-1)} \cos [\alpha_{jn}(\ell_n - x)/\ell_n]\} \csc \alpha_{jn} \tag{25}$$

and, in particular,

$$S_{jn}(\ell_n) = \omega \rho_{jn} A_{jn} \beta_{jn} (U_{jn} \cot \alpha_{jn} - U_{j(n-1)} \csc \alpha_{jn}) \tag{26a}$$

$$S_{jn}(0) = \omega \rho_{jn} A_{jn} \beta_{jn} (U_{jn} \csc \alpha_{jn} - U_{j(n-1)} \cot \alpha_{jn}) \tag{26b}$$

The equations of motion for the link masses m_{1n} and m_{2n} are given by

$$-\omega^2 m_{1n} U_{1n} = k_n^* (U_{2n} - U_{1n}) + S_{1(n+1)}(0) - S_{1n}(\ell_n) \tag{27a}$$

$$-\omega^2 m_{2n} U_{2n} = k_n^* (U_{1n} - U_{2n}) + S_{2(n+1)}(0) - S_{2n}(\ell_n) \tag{27b}$$

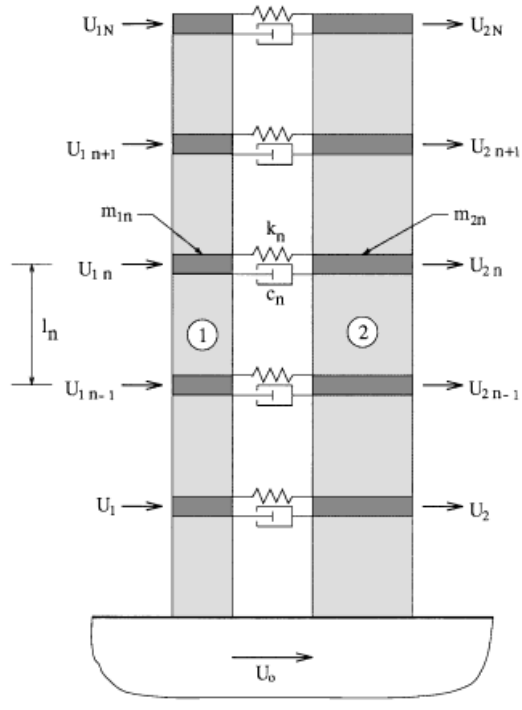

Figure 12. Schematic representation of composite structure showing shear beams connected by flexible links

for $1 \leqslant n \leqslant N-1$ and

$$-\omega^2 m_{1N} U_{1N} = k_N^*(U_{2N} - U_{1N}) - S_{1N}(\ell_N) \tag{28a}$$

$$-\omega^2 m_{2N} U_{2N} = k_N^*(U_{1N} - U_{2N}) - S_{2N}(\ell_N) \tag{28b}$$

for $n = N$.

Substitution from equations (26a) and (26b) into equations (27a), (27b), (28a) and (28b) leads to the following system of equations for U_{1n}, U_{2n} $(n = 1, N)$:

$$(\bar{k}_N^* - a_0^2 c_{1N} + b_{1N})\, U_{1N} - \bar{k}_N^* U_{2N} - a_{1N} U_{1(N-1)} = 0 \tag{29a}$$

$$-\bar{k}_N^* U_{1N} + (\bar{k}_N^* - a_0^2 c_{2N} + b_{2N})\, U_{2N} - a_{2N} U_{2(N-1)} = 0 \tag{29b}$$

$$-a_{1(n+1)} U_{1(n+1)} + (\bar{k}_n^* - a_0^2 c_{1n} + b_{1n} + b_{1(n+1)}) U_{1n} - \bar{k}_n^* U_{2n} - a_{1n} U_{1(n-1)} = 0$$

$$(2 \leqslant n \leqslant N-1) \tag{29c}$$

$$-a_{2(n+1)} U_{2(n+1)} - \bar{k}_n^* U_{1n} + (\bar{k}_n^* - a_0^2 c_{2n} + b_{2n} + b_{2(n+1)}) U_{2n} - a_{2n} U_{2(n-1)} = 0$$

$$(2 \leqslant n \leqslant N-1) \tag{29d}$$

and

$$-a_{12}U_{12} + (\bar{k}_1^* - a_0^2 c_{11} + b_{11} + b_{12})U_{11} - \bar{k}_1^* U_{21} = a_{11}U_0 \tag{29e}$$

$$-a_{22}U_{22} - \bar{k}_1^* U_{11} + (\bar{k}_1^* - a_0^2 c_{21} + b_{21} + b_{22})U_{21} = a_{21}U_0 \tag{29f}$$

where U_0 is the prescribed motion of the base and

$$a_0 = \frac{\omega \bar{\ell}}{\bar{\beta}} \tag{30a}$$

$$\bar{k}_n^* = \frac{k_n^*}{(\bar{\rho}\bar{A}\bar{\beta}^2/\bar{\ell})} = \bar{k}_n \left[1 + 2\mathrm{i}a_0\, \xi_{n\ell\mathrm{v}}/\sqrt{\bar{k}_n}\right] \tag{30b}$$

$$a_{jn} = \left(\frac{\omega\bar{\ell}}{\bar{\beta}}\right)\left(\frac{\rho_{jn}A_{jn}\beta_{jn}}{\bar{\rho}\bar{A}\bar{\beta}}\right)\csc\alpha_{jn} \tag{30c}$$

$$b_{jn} = \left(\frac{\omega\bar{\ell}}{\bar{\beta}}\right)\left(\frac{\rho_{jn}A_{jn}\beta_{jn}}{\bar{\rho}\bar{A}\bar{\beta}}\right)\cot\alpha_{jn} \tag{30d}$$

$$c_{jn} = \left(\frac{m_{jn}}{\bar{\rho}\bar{A}\bar{\ell}}\right) \tag{30e}$$

in which $\bar{\rho}$, $\bar{A}$, $\bar{\beta}$ and $\bar{\ell}$ are a density, cross-sectional area, shear-wave velocity and length of the reference. In equation (30b), $\bar{k}_n = k_n\bar{\ell}/\bar{\rho}\bar{A}\bar{\beta}^2$ is a dimensionless link stiffness constant and $\xi_{n\ell\mathrm{v}}$ is related to the viscous damping constants in the links.

Equations (29) allow us to calculate the displacements U_{1n} and U_{2n} at all links. The displacements and shear forces within each shear beam can then be calculated by using equations (24) and (25). This formulation appears to be accurate for a wide range of values of $\bar{k}_n$. An alternative formulation based on transfer matrices similar to that used for the case of rigid links suffers from ill-conditioning as $\bar{k}_n$ becomes large. Once the response in the frequency domain has been calculated, the response in the time domain can be obtained by Fourier synthesis.

Results in the frequency domain

The effects of the flexibility of the links between two uniform shear beams interconnected by five equally spaced links are illustrated in Figures 13 and 14. The structure is characterized by $\bar{\beta}_1 = 309$ m/sec, $\bar{\beta}_2 = 48$ m/sec, $\bar{\beta} = \beta_e = 160$ m/sec, $\mu_1 = 0{\cdot}25$, $\mu_2 = 0{\cdot}75$, $\xi_{1\mathrm{s}} = \xi_{2\mathrm{s}} = 0{\cdot}02$, $\xi_{2\mathrm{v}} = 0{\cdot}03$, $H = 200$ m, $N = 5$ and $\bar{\ell} = \ell_n = 40$ m and corresponds to a model of a 50-storey building. The links are assumed massless ($m_{1n} = m_{2n} = 0$). Results for the amplitude of the transfer functions $U_{1N}(\omega)/U_0$ and $U_{2N}(\omega)/U_0$ ($N = 5$) for the absolute displacement at the top of the external and internal structures are shown for three values of the normalized stiffness of the links ($\bar{k}_n = \bar{k} = 1{\cdot}0$, $0{\cdot}1$ and $0{\cdot}01$) and for three values ($\xi_{\ell\mathrm{v}} = 0{\cdot}0$, $0{\cdot}05$ and $0{\cdot}10$) of the normalized viscous damping $\xi_{\ell\mathrm{v}}$ on the links. The results for $\bar{k} = 1{\cdot}0$ are close to those for a rigid link ($\bar{k} = \infty$) while those for $k = 0{\cdot}01$ and $\xi_{\ell\mathrm{v}} = 0{\cdot}0$ essentially represent the case of an internal structure uncoupled from the external structure.

The results in Figure 13(a) indicate that as the stiffness of the links is reduced the fundamental frequency of the composite structure and the peak amplitude for the response of the external structure in the fundamental mode are reduced. Unfortunately, in the absence of damping in the links, the response in a second mode is drastically increased as the links become more flexible (Figure 13(a)). By introducing damping in the links,

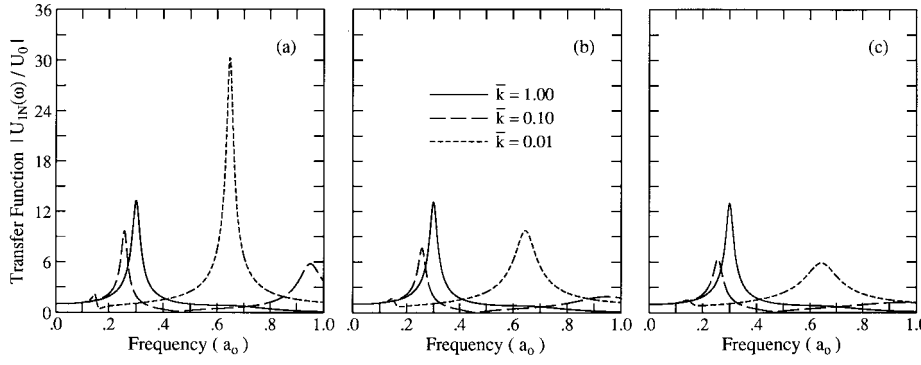

Figure 13. Amplitude of the transfer function $U_{1N}(\omega)/U_0$ at the top of the external structure of a 50-storey composite building for different values of the normalized link stiffness $\bar{k}$ and for link damping ratios $\xi_{\ell v} = 0{\cdot}0$ (a), 0·05 (b) and 0·10 (c)

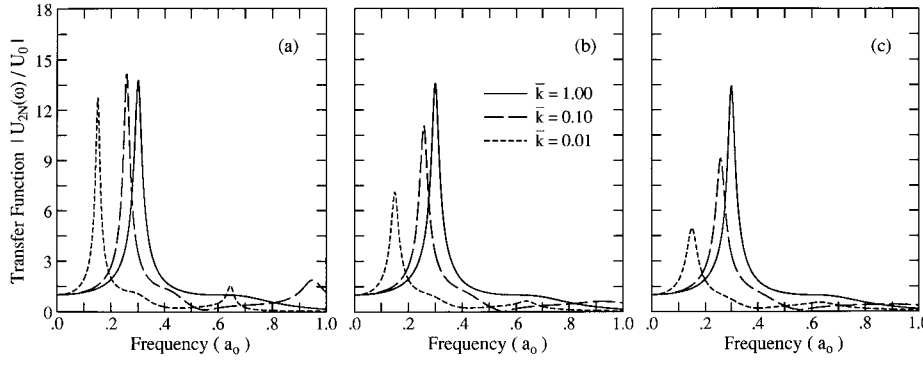

Figure 14. Amplitude of the transfer function $U_{2N}(\omega)/U_0$ at the top of the internal structure of a 50-storey composite building for different values of the normalized link stiffness $\bar{k}$ and for link damping ratios $\xi_{\ell v} = 0{\cdot}0$ (a), 0·05 (b) and 0·10 (c)

the response of the external structure on this second mode can be reduced (Figure 13(b) and 13(c)). When no damping is provided in the links ($\xi_{\ell v} = 0{\cdot}0$), the peak amplitude of the response of the internal structure in the fundamental mode is not changed substantially as the links are made more flexible (Figure 14(a)). The introduction of damping in the links also reduces the response of the internal structure (Figures 14(b) and 14(c)).

Results in the time domain

To illustrate the results of time-domain calculations for a structure modelled as two shear beams interconnected by flexible links we consider a 50-storey building consisting of five segments ($N = 5$) characterized by the following properties: $\bar{\ell} = \ell_n = 40$ m, $\xi_{1s} = \xi_{2s} = 0{\cdot}02$, $\xi_{2v} = 0{\cdot}03$, $\rho_1 A_1/\bar{\rho}\bar{A} = 0{\cdot}20$, $\rho_2 A_2/\bar{\rho}\bar{A} = 0{\cdot}65$, $c_{1n} = 0{\cdot}05$, $c_{2n} = 0{\cdot}10$, $\mu_1 = (\rho_1 A_1/\bar{\rho}\bar{A}) + c_{1n} = 0{\cdot}25$, $\mu_2 = (\rho_2 A_2/\bar{\rho}\bar{A}) + c_{2n} = 0{\cdot}75$, $\bar{\beta}_2/\beta_e = 0{\cdot}30$ and $\bar{\beta}_1/\beta_e = 1{\cdot}931$. The structure is subjected to the NS El Centro 1940 excitation. For the links we consider two sets of properties. The first case, representing fairly stiff links, is characterized by $\bar{k}_n = 1{\cdot}0$ and $\xi_{n\ell v} = 0{\cdot}10$. In this case, we select $\bar{\beta} = \beta_e = 160$ m/sec. The second case, representing very flexible links, is defined by $\bar{k}_n = 0{\cdot}05$ and $\xi_{n\ell v} = 0{\cdot}10$. In this case, to maintain the same fundamental frequency as in the first case, we select $\bar{\beta} = \beta_e = 200$ m/sec.

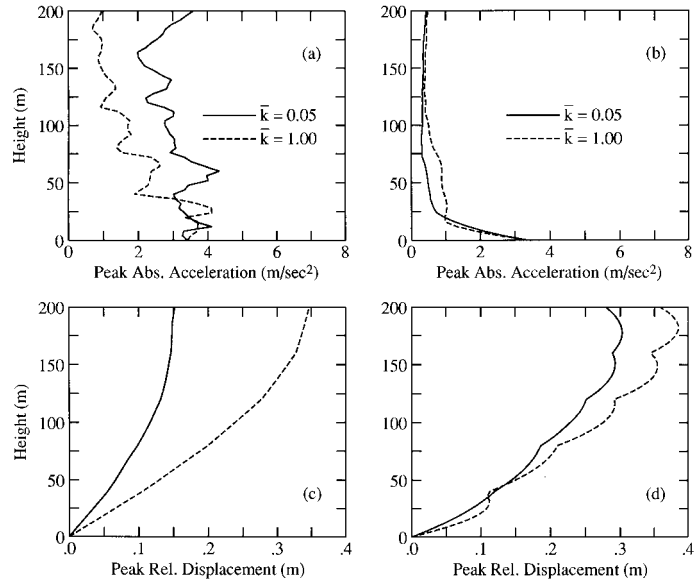

Figure 15. Distribution of peak absolute acceleration (m/sec^2) and peak displacement relative to the base (m) along the height of the external ((a), (c)) and internal ((b), (d)) structures in a composite 50-storey building with flexible links

The profiles of peak absolute accelerations and peak displacements relative to the base along the height of the external ($j = 1$) and internal ($j = 2$) structures are presented in Figure 15. Considering first the response along the external structure we see that the softening of the links results, in this case, in an increase of the absolute acceleration (Figure 15(a)) and in reductions of the relative displacement with respect to the base (Figure 15(c)). For the internal structure, the softening of the links results in reductions of the absolute accelerations (Figure 15(b)) and displacements relative to the base (Figure 15(d)).

If we compare the results for a composite 50-storey structure with flexible links ($\bar{k} = 0{\cdot}05$, $\xi_{n\ell v} = 0{\cdot}10$) and an internal structure characterized by $\bar{\beta}_2/\beta_e = 0{\cdot}30$ and $\xi_{2v} = 0{\cdot}03$ (Figure 15), with those for a 50-storey structure with rigid links ($\bar{k} = \infty$) and a more flexible internal structure such that $\bar{\beta}_2/\beta_e = 0{\cdot}10$ and $\xi_{2v} = 0{\cdot}008$ (Figure 8, Case 1), we find that the peak accelerations of the internal structure in the vicinity of the links are lower for the structure with the flexible links. The peak displacements relative to the base in the internal structure are increased for the case of a stiffer internal structure with flexible links. Finally, in the case of flexible links, the peak inter-storey displacements are reduced.

CONCLUSIONS

It has been shown that a structural system consisting of a stiff and lightly damped external structure connected at a few locations along the height to a flexible and moderately damped internal structure can lead to a significantly lower seismic response than the more common structural configurations. In the mixed configuration, the internal structure plays the role of a mass damper for the external structure.

If the links between the internal and external structures are very stiff, significant response reductions can only be obtained if the internal structure is made very flexible and if the added viscous damping within the internal structure is kept at or close to the optimal values. The reductions of the absolute accelerations, absolute velocities and displacements relative to the base apply to both the external and internal structures but are gained at the expense of significant inter-floor deformations of the internal structure. These inter-floor deformations can be limited by judiciously increasing the added viscous damping.

As the height of the building and the number of segments of the internal structure are increased, the flexibility of the internal structure must be increased to obtain significant overall response reductions.

Flexible and damped links between the internal and external structures can be used to reduce the requirement of extremely flexible internal structures. In this case, significant response reductions for the internal structure can be gained at the expense of smaller reductions of the response of the external structure. If flexible links are used, it is necessary to provide for additional damping at the links.

ACKNOWLEDGEMENT

This work was supported by a Grant from the Ohsaki Research Institute of Shimizu Corporation.

REFERENCES

1. A. Mita and M. Kaneko, 'Vibration control of tall buildings utilizing energy transfer into sub-structural systems', *Proc. 1st World Conf. on Structural Control*, 3–5 August 1994, Pasadena, CA, TA2-31/TA2-40.
2. A. Mita and M. Q. Feng, 'Response control strategy for tall buildings using interaction between mega- and sub-structures', *Proc. Int. Workshop on Civil Infrastructural Systems*, Taipei, Taiwan, Republic of China, 1994, pp. 329–341.
3. H. Yokota, M. Saruta, Y. Nakamura, N. Satake, K. Okada, Y. Ogawa and Y. Fujita, 'Structural control for seismic loads using viscoelastic dampers', *Proc. 10th World Conf. on Earthquake Engineering*, July 1992, Madrid, Spain, Vol. 4, 1992, pp. 2441–2446.
4. K. Gurley, A. Kareem, L. A. Bergman, E. A. Johnson and R. E. Klein, 'Coupling tall buildings for control of response to wind', *Proc. Int. Conf. on Structural Safety and Reliability*, '*93* (*ICOSSAR*), A. A. Balkema Publishers, Rotherdam, 1994, pp. 1553–1560.
5. J. E. Luco and F. C. P. de Barros, 'Active and passive control of the dynamic response of tall buildings', *Report*, Department of Applied Mechanics and Engineering Sciences, University of California, San Diego, La Jolla, California, September 1994, 130pp.

